Organic & Biomolecular Chemistry

Cite this: *Org. Biomol. Chem.*, 2012, **10**, 6333

www.rsc.org/obc

PAPER

Theoretical study on the hypervalent λ^3-bromane strategy for Baeyer–Villiger oxidation of benzaldehyde and acetaldehyde: rearrangement mechanism†

Hui Fu,*[a,b] Shouwen Xie,[b] Aiping Fu,[c] Xufeng Lin,[a,b] Hui Zhao[a] and Tianxu Ye[b]

Received 14th March 2012, Accepted 8th June 2012
DOI: 10.1039/c2ob25551k

The rearrangement mechanisms of the novel Baeyer–Villiger oxidation (BVO) of benzaldehyde and acetaldehyde have been studied using density functional theory methods. All structures associated with the product formation step of the new Criegee intermediate, α-hydroxyalkoxy-λ^3-bromane, are reported. B3LYP/6-31++G** calculations give a good description for the group shift of these two typical reactants: phenyl shift is easier than hydrogen shift for benzaldehyde; hydrogen migration is more favorable than methyl migration for acetaldehyde. Different mechanisms and various conformers of the novel BVO reaction have been considered for the migration step. Solvent effects and rate constants are also taken into account. The calculated and experimentally observed branching ratios are in good agreement with each other.

Introduction

The Baeyer–Villiger (BV) reaction, in which ketones are converted into esters or lactones,[1] is of great significance in organic synthesis due to its excellent regioselective and stereoselective control. As a result, it has been extensively studied experimentally and theoretically for more than 100 years and is still the subject of many publications.[2–11]

The basic mechanism of the BV reaction has been well known since 1948.[12] The first step is the carbonyl addition of a peroxyacid to a ketone, producing a tetrahedral adduct known as the Criegee intermediate. The second step is the migration of the alkyl or aryl group from the ketone moiety to the nearest peroxide oxygen in the intermediate. The latter step is concerted with retention of stereochemistry of the migrating group and is rate-limiting in the vast majority of cases.[13] The regiospecificity of the reaction depends on the relative migratory ability of the substituents attached to the carbonyl group. Substituents which are able to stabilize a positive charge migrate more readily, so that the order of preference is *tert*-alkyl > cyclohexyl > *sec*-alkyl > phenyl > primary-alkyl > CH_3.[6] In some cases, stereoelectronic or ring strain factors also affect the regiochemical outcome. In classical BV reaction, the reaction of an aldehyde preferentially gives formates; however, some aldehydes may be exceptions due to the solvolytic instability of the formate product under the reaction conditions, such as *p*-ClC_6H_4CHO and PhCHO.[2,3,14,15]

Although the classical BV reaction was studied extensively, in 2010, Ochiai *et al.*[16] reported a novel strategy for this reaction, and a three-step mechanism has been proposed (Scheme 1). This novel method involves hydration of carbonyl compounds in the first step, followed by a ligand exchange of hypervalent aryl-λ^3-bromane with the resulting hydrate (*gem*-diol), producing a new Criegee intermediate α-hydroxyalkoxy-λ^3-bromane. The last step is the migration of a hydrogen atom or an alkyl (aryl) group in the new Criegee intermediate from the carbon atom to the oxygen atom, producing RCOOH or ROOCH. According to Ochiai's study, the new methodology makes it possible to induce selectively the BV rearrangement of straight chain primary aliphatic as well as aromatic aldehydes, which is missing in the classical BV.[16]

Obviously, according to the hypothetical mechanism of Ochiai for the new strategy of the BV reaction, the last migration step is the critical step because it determines the type of the product, *i.e.* whether R_1 or R_2 migrates from the C to O atom. In their experiment for most of the aldehydes, the migration of an alkyl (aryl) group is easier than hydrogen, which makes the ester the major product. A typical example is the BV reaction of benzaldehyde (where R_1 = H, R_2 = phenyl in Scheme 1), whose only product is PhOCOH. This implies that only the phenyl shift is occurring in its new Criegee intermediate under the experimental conditions. However, there is another interesting observation for the new type of BV reaction: for acetaldehyde (where R_1 = CH_3, R_2 = H in Scheme 1). The primary product is acetic

[a]*State Key Laboratory of Heavy Oil Processing, China University of Petroleum, Shandong, Qingdao 266555, People's Republic of China. E-mail: fuhui@upc.edu.cn*
[b]*College of Science, China University of Petroleum, Shandong, Qingdao 266555, People's Republic of China*
[c]*Laboratory of New Fiber Materials and Modern Textile, Growing Base for State Key Laboratory, Qingdao University, Shandong, Qingdao 266071, People's Republic of China*

†Electronic supplementary information (ESI) available. See DOI: 10.1039/c2ob25551k

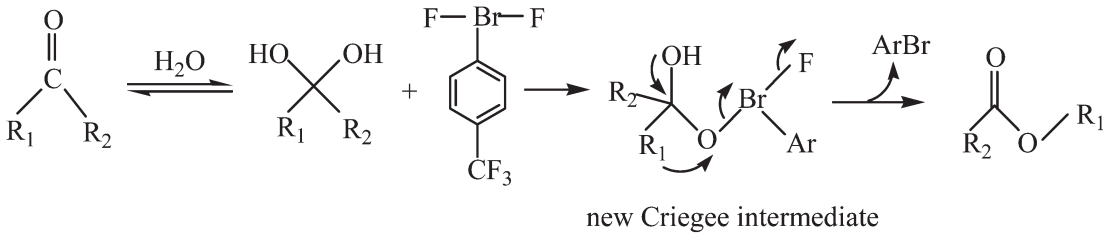

Scheme 1 Ligand exchange pathway to the Criegee intermediate.[16]

acid in high yield (95%) instead of methyl formate ester. Our interest in the above phenomenon prompted us to carry out a theoretical investigation of the BV reactions using benzaldehyde and acetaldehyde.

Due to the importance of the BVO reaction in organic synthesis, several computational attempts have been conducted in the literature for the classical BVO reactions.[5–11] They include the rate coefficient,[9] the substituent effects,[10] the solvent effects,[11] the role of hydrogen bonding,[6] and so on. For the computational investigations of this novel strategy of the BVO reaction, only Ochiai *et al.*[16] have reported a migration mechanism involving the protonated α-hydroxyethoxy-λ^3-bromane in the gas phase using MP2 method. However, their computational results could not be compared to their experimental results. Alvarez-Idaboy *et al.*[9] have reported that compared to the MP2 method, DFT methods could provide a good qualitative description of the BVO reaction mechanism. Thus, in this work, the new-type BVO reactions of benzaldehyde and acetaldehyde were investigated by means of DFT methods, and the solvent effect was also considered.

Computational details

All calculations were performed with the Gaussian 03 program package.[17] The geometries were located by using B3LYP, a hybrid DFT method.[18–21] The 6-31++G** basis set[5] was employed throughout. The transition state (TS) was characterized by vibrational analysis in order to confirm that it has only one imaginary frequency. From the transition state, the reaction path was traced by the IRC to ensure the correctness of the transition state. Furthermore, by means of the CPCM continuum solvation model[22,23] with UFF radii,[9,24,25] the solvent effect was considered through single-point energy calculations with the same calculation level. Dichloromethane (ε = 8.93) has been chosen as a common solvent for the BVO reaction.[5–11,16] The Gibbs free energies in the solvent ($G_{solvent}$) were calculated by adding the total energy in the solvent ($E_{solvent}$) and the gas-phase thermal correction to the Gibbs free energy (TCG_{gas}) at 298.15 K.[11] The charge distribution in the intermediates has been analyzed *via* natural population analysis (NPA).[26–30] The CCSD(T)[31] single point calculation was performed and the results are consistent with the B3LYP results. That is to say, the DFT calculation in our paper is reliable.

In order to clearly describe the last step of this novel BVO reaction, the Gibbs free energy changes of all structures in the migration step were obtained from the frequency calculation, and the rate constants in this reaction were calculated using classical transition state theory (TST) by eqn (1):[32,33]

$$k(T) = \frac{k_B T}{h} \exp\left(-\frac{\Delta G^{\neq}}{RT}\right) \quad (1)$$

where $\Delta G^{\neq}$, k_B, h, T, R denote the Gibbs free energy of activation, Boltzmann's constant, Planck's constant, the temperature and the universal gas constant, respectively.

Results and discussion

3.1 Mechanism description

The mechanism of this new BVO reaction contains three steps as indicated in Scheme 1.[16] The last step determines the type of major product. Thus, the work in this paper focused on the last step. In this step, Ochiai *et al.* divided it into two parts. In the first part, the status of bromine changes from Br(III) to Br(II) accompanied by elimination of hydrogen fluoride from the new intermediate. And a hydrogen bond is formed between the fluoride and the hydroxyl hydrogen in the aldehyde. The second part involves the hydrogen or alkyl (aryl) shift from the carbon of the hemiacetal group to the nearest oxygen, approaching bromine. This part produces the acid or ester as well as bromobenzene. The valence of bromine converts from Br(II) to Br(I) in this part. This two-part step could be treated as stepwise mechanism.

An alternative mechanism of the last step in this BVO reaction has been proposed in our work. The activated intermediate directly generates a protonated acid or ester *via* hydrogen or alkyl (aryl) shift accompanied with HF and PhBr formation. And similarly with the stepwise mechanism, the migrating group also shifts from the carbon of the hemiacetal group to the nearest oxygen, approaching bromine in this mechanism. At the same time, the valence of bromine changes from Br(III) to Br(I). Subsequently, the protonated acid or ester interacts with HF through hydrogen bonding, which weakens the interaction between the proton and acid (ester). Thus, this process will contribute to the generation of acid and ester. This one-part step could be defined as concerted mechanism.

For aldehydes, the new Criegee intermediate has two conformers in *anti* and *syn* arrangement, because of the different relative positions between the phenyl combining with bromine and the OH connected to the carbon of the hemiacetal. The protonated new Criegee intermediate does not change the stereochemistry.

3.2 The mechanism of the novel BVO rearrangement of benzaldehyde

3.2.1 Stepwise mechanism. The free energy profile and all structures of the *anti* conformer in the stepwise mechanism are shown in Fig. 1 (black and red line) and 2, respectively.

For phenyl migration (black line in Fig. 1), in the first part of the stepwise mechanism, the valence of bromine changes from Br(III) in **1a** to Br(II) in **2a** and a H2F···H1O1 hydrogen bond (1.942 Å) forms with a free energy barrier of 8.17 kJ mol^{-1}.

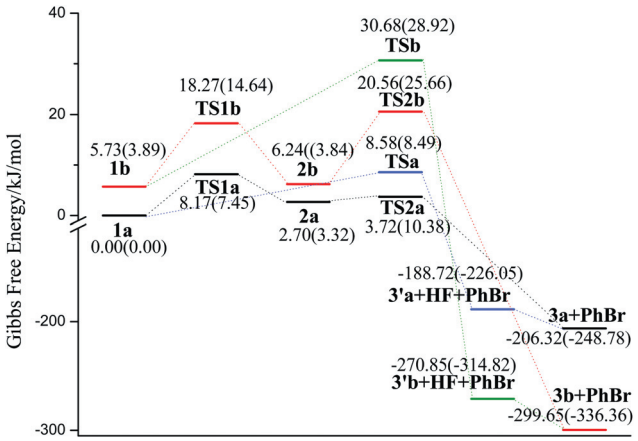

Fig. 1 Calculated free energy profile for the group migration of protonated *anti*-α-hydroxybenzyloxy-λ^3-bromane phenyl migration (stepwise mechanism in black line and concerted mechanism in blue line) and H migration (stepwise mechanism in red line and concerted mechanism in green line), using DFT (B3LYP/6-31++G**) method. The values in parentheses correspond to the single point calculation in dichloromethane.

In addition, part (1) in Fig. 2 shows that the C1–C bond slightly increases with the decrease of the C1···O distance, as well as the increase of the Br–O bond length. This may be conducive to the phenyl shift and PhBr formation in the next step. In the second step, the C–C1 σ bond is cleaved and the C1–O σ bond is formed. Structure **2a** produces **3a** (complex of HF and protonated PhOCOH) and PhBr *via* 1,2-phenyl shift with a free energy barrier of 1.02 kJ mol^{-1}. Additionally, IRC calculation and vibration analysis also verified the correctness of the transition state. The calculated free energy barrier of the 1,2-phenyl shift is very small, which is consistent with the fact that the phenyl shift can easily occur.

For H migration (red line in Fig. 1 and part (2) in Fig. 2), a similar process takes place. For the second step, intermediate **2b** produces **3b** (complex of HF and protonated PhCOOH) and PhBr *via* a 1,2-H shift (*via* TS2b) with a free energy barrier of 14.32 kJ mol^{-1}. This is higher than the phenyl shift. It illustrates that the formation of ester is much easier than the formation of carboxylic acid, which explains well the experimental observation.[16]

As mentioned above, the 1,2-phenyl shift is much easier than the hydrogen shift. This phenomenon can be interpreted in terms of electronic effects. The percent group migration seems to depend primarily on the electron-donor ability of the migrating groups. In this reaction, the rate of the 1,2-shift of an alkyl group to the electron-deficient oxygen atom attached to bromine in the new Criegee intermediate increases with the increase in the electron-donating power of the migrating group.[34] Similar electronic effects of the alkyl substituent were reported in the classical BVO of methyl ketone by permaleic acid and trifluoroperacetic acid.[35] From the migrating moiety point of view, it is well known that the electron-donating power of phenyl is stronger

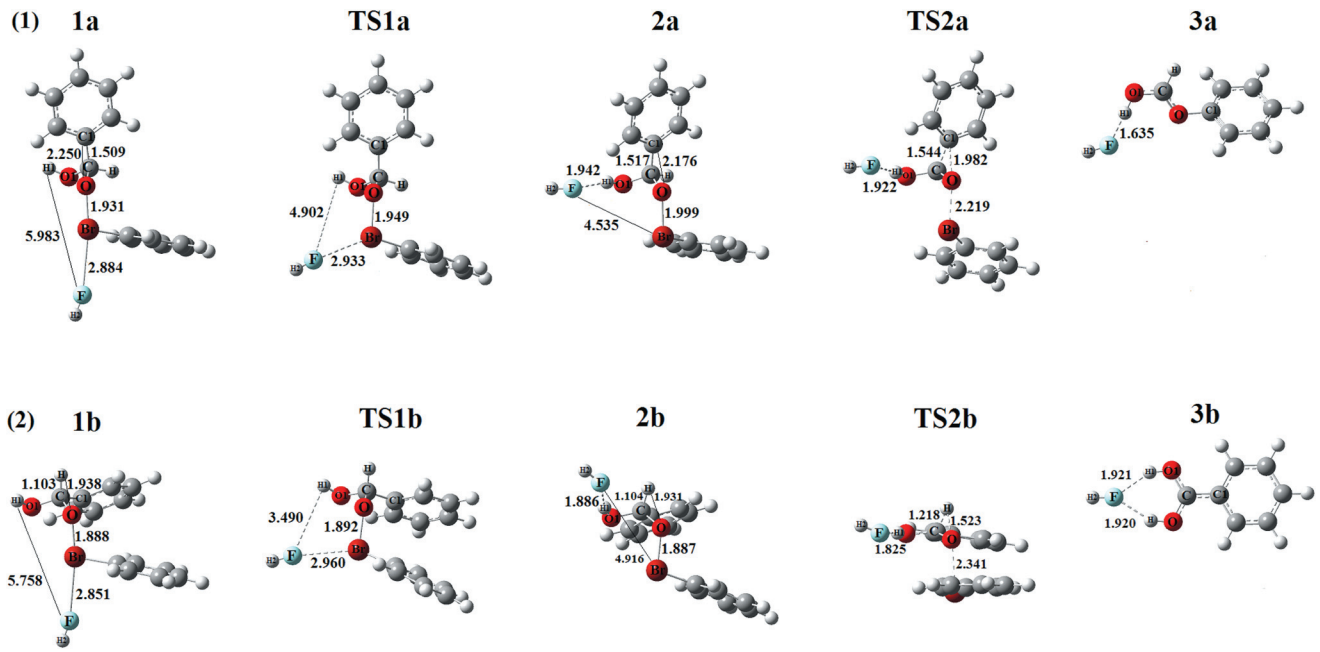

Fig. 2 Structures of intermediates, transition states, and products of stepwise mechanism of protonated *anti*-α-hydroxybenzyloxy-λ^3-bromane, using DFT (B3LYP/6-31++G**) methods: phenyl migration (above) and hydrogen migration (below). **1a**(**1b**): protonated *anti*-α-hydroxybenzyloxy-λ^3-bromane, **3a**(**3b**): complex of HF and protonated PhOCOH (PhCOOH). The distances are in Å.

than hydrogen. Furthermore, phenyl stabilizes the positive charge more readily. Therefore, the phenyl-migration is easier than the H-migration.

In experiment, because this novel BVO is carried out in dichloromethane, the solvent effect on the group shift was also examined with the prior conformer (*anti* conformer), see the values in parentheses in Fig. 1. All calculated results in dichloromethane are compatible with the experimental observations of the preferred formation of PhOCOH over PhCOOH production[16] and consistent with the results in the gas phase.

The stepwise mechanisms of the *syn* conformer of benzaldehyde (see Fig. S1 and S2 in the ESI†) were also investigated. The results also show that the phenyl shift occurs more favorably compared with the hydrogen shift. Compared with the *anti* conformer, it was found that the *syn* conformers are not favorable for the stepwise mechanism.

3.2.2 Concerted mechanism. The free energy profiles and all the structures of benzaldehyde in the *anti* conformer in the concerted mechanism are presented in Fig. 1 and 3 (blue and green line).

For phenyl migration (blue line in Fig. 1), the protonated PhOCOH can be generated with a free energy barrier of 8.58 kJ mol^{-1} *via* a 1,2-phenyl shift. The phenyl group can donate electrons to stabilize the electron-deficient oxygen with the cleavage of the C–C1 bond and formation of the C1–O bond. At the same time, bromobenzene and HF are also formed. The geometric changes shown in Fig. 3 also illustrate the trend in group migration. Subsequently, the protonated PhOCOH forms a hydrogen bond with HF, which leads to the increase of the O1–H1 bond length. Thus, the formation of a hydrogen bond can weaken the interaction between H1 and O1 (see Fig. 3), which helps the formation of the final product, ester or acid.

The H migration (green line in Fig. 1) involves hydrogen migration with the formation of protonated PhCOOH. The free energy barrier of this process is 24.95 kJ mol^{-1}, which is much higher than that of phenyl migration. It indicates that the hydrogen shift is more difficult than the phenyl shift in the concerted mechanism. This trend is similar to the trend of group migration for the same reason as the stepwise mechanism.

The solvent effect was also examined for the concerted mechanism, as can be seen in Fig. 1 (the values in parentheses). All of the calculated results in dichloromethane are consistent with the above study in the gas phase.

Furthermore, the concerted mechanism for benzaldehyde in the *syn* conformers (see Fig. S1 and S3†) was also calculated. The results show that the phenyl shift is more favorable than the hydrogen shift. Compared with the *anti* conformer, *syn* conformers are not favorable.

By comparison of the two mechanisms of the *anti* conformer, one can see that the hydrogen shift in the stepwise mechanism is obviously more favorable than in the concerted mechanism. In contrast to that the phenyl shift does not show obvious favorability. It is well known that the electron-deficiency of oxygen connected to bromine should benefit group migration. The NPA charge analysis may interpret this phenomenon. The O atom in structure **2b** bears a negative charge of −0.559 in the stepwise mechanism, which is less than that of the O atom (−0.571) in structure **1b** in the concerted mechanism. The less negative charge of O is conducive to H migration. Therefore, the stepwise mechanism is more likely prone to hydrogen migration reaction. The same charge change on the O atom can be found in the

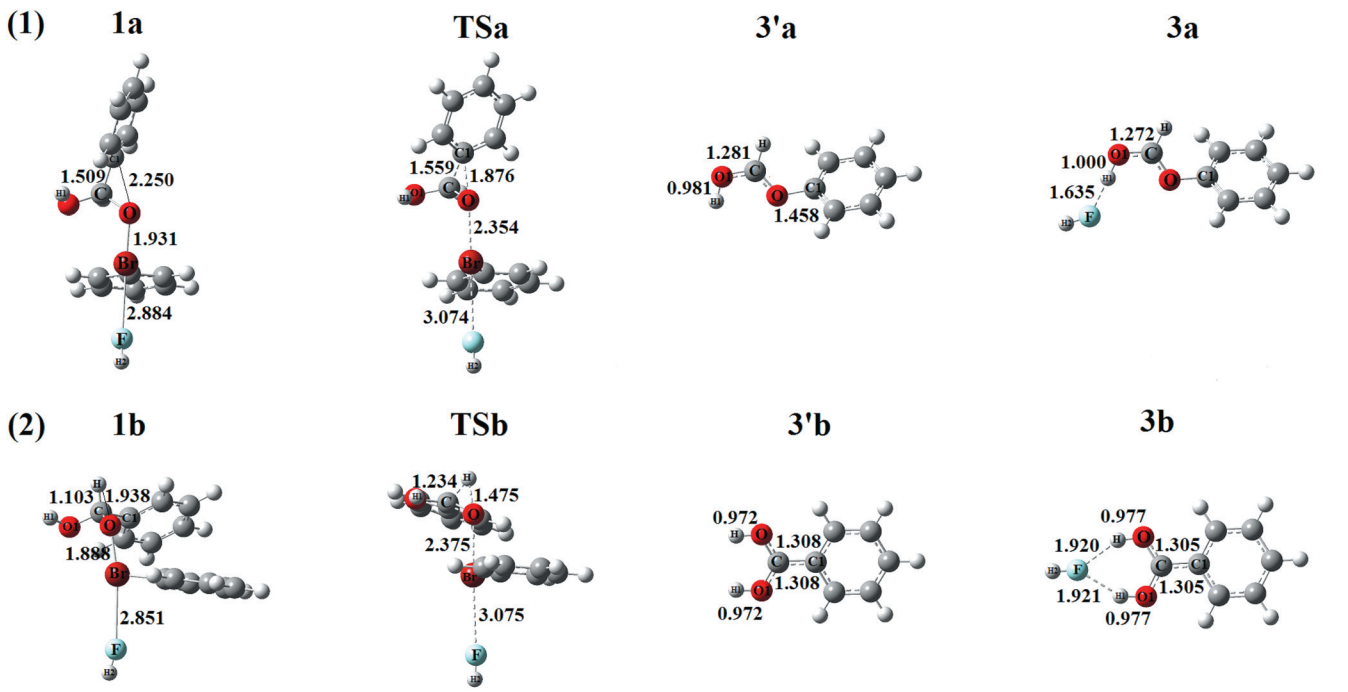

Fig. 3 Structures of intermediates, transition states, and products of the concerted mechanism of protonated *anti*-α-hydroxybenzyloxy-λ^3-bromane, using DFT (B3LYP/6-31++G**) methods: phenyl migration (above) and hydrogen migration (below). **1a**(**1b**): protonated *anti*-α-hydroxybenzyloxy-λ^3-bromane, **3a**(**3b**): complex of HF and protonated PhOCOH (PhCOOH). The distances are in Å.

phenyl migration. However, the charges on the Br atoms with different mechanisms are obviously different to each other (0.533 in TS2a and 0.448 in TSa, respectively) for the phenyl migration. In contrast to that, the charges of Br atoms with different mechanisms are quite close (0.402 in TS2b and 0.404 in TSb) for the H migration. The effect of the great difference on Br atom may lead to competition between the two mechanisms in phenyl migration.

3.2.3 Rate constants and branching ratio. According to Ochiai's experimental results,[16] the rate-limiting step in dichloromethane is the moiety shift. Hence, in order to better understand this novel BVO reaction, the rate constants of the group shift step were examined in dichloromethane for the favorable stepwise mechanism at 298.15 K. Calculated energetic results were used for the TST equation given in the calculation details. For the phenyl migration, the forward rate constant is 9.43×10^{10} s^{-1} and the reverse rate constant is 2.48×10^{-33} mol^{-1} dm^3 s^{-1} at 298.15 K. In contrast to that, for the hydrogen migration, the forward rate constant is 9.54×10^{8} s^{-1} and the reverse rate constant is 2.38×10^{-51} mol^{-1} dm^3 s^{-1} at 298.15 K.

From the above results, for either the phenyl or the hydrogen shift, the reverse reactions are difficult to undertake, and the forward rate constant of the phenyl shift is about two orders of magnitude higher than that of the hydrogen shift. These results also illustrate that PhOCOH is likely to be formed, which is also consistent with the experimental observations.[16]

Additionally, to further verify the reliability of the above computational results, the difference in the calculated Gibbs free energy of activation ($\Delta\Delta G^{\neq}$) has been used to predict the branching ratio from absolute rate theory, by $\ln(k_{PhOCOH}/k_{PhCOOH}) = \Delta\Delta G^{\neq}/RT$. Table 1 lists the corresponding branching ratio and $\Delta\Delta G^{\neq}$ values in the gas phase and in dichloromethane, and they are compared with the available experimental data.[16] There is an excellent agreement between the calculated and experimental values.

3.3 The mechanism of the novel BVO rearrangement of acetaldehyde

3.3.1 Stepwise mechanism. Fig. 4 and 5 display the free energy profile and the critical structures of the stepwise mechanism for the *anti* conformer, for the BVO rearrangement of acetaldehyde.

For the CH_3 migration (see black line in Fig. 4 and part (1) in Fig. 5), firstly, the valence of bromine changes from Br(III)(**1c**) to Br(II)(**2c**) accompanied by the formation of the H1···F hydrogen bond. The stereochemistry of **2c** does not change in this step. The free energy barrier is 11.39 kJ mol^{-1}. Secondly, the methyl shifts from C to O. This process (**2c** to TS2c) is endothermic by 36.78 kJ mol^{-1}.

For H migration (red line in Fig. 4 and part (2) in Fig. 5), a similar process was also examined. The H migration needs the free energy of activation of 27.69 kJ mol^{-1}, which is much lower than the methyl shift. Thus, it can be concluded that hydrogen migration is easier than methyl migration, which is consistent with the experimental observation for the preferred formation of acetic acid over methyl formate.[16]

Generally, the electron-donating power of methyl is slightly stronger than hydrogen, therefore, the methyl migration should be easier than hydrogen migration. However, interestingly, experimental observation[16] seems to be inconsistent with the above hypothesis. Our calculated results were compatible with experimental observations. This anomalous phenomenon could be explained by the following reasons. Firstly, this reaction involves σ bond breaking, and then the methyl anion or the hydrogen anion migrates from C to O. Hydrogen anion is more stable than methyl anion which illustrates that it is more favorable to form the hydrogen anion than the methyl anion, thus, the required free energy for forming the hydrogen anion is also lower than that of the methyl anion. Another reason could be the stability of the carbocation in the process of σ bond breaking: the carbocation formed from hydrogen migration is more stable than that formed from methyl migration. In summary, hydrogen migration is easier than methyl.

In order to verify the rationality of the computational method, single point calculation was done with the MP2 method at the same basis set with B3LYP. Our calculated MP2 results indeed lifted the energy barrier, and changed the order of group migration as in Ochiai's work.[16] While the single point

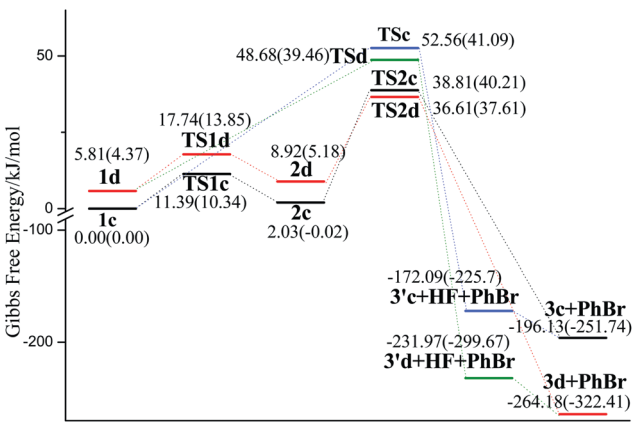

Fig. 4 Calculated free energy profile for group migration of protonated *anti*-α-hydroxyethoxy-λ³-bromane: CH_3 migration (stepwise mechanism in black line and concerted mechanism in blue line) and H migration (stepwise mechanism in red line and concerted mechanism in green line), using DFT (B3LYP/6-31++G**) method. The values in parentheses correspond to the single point calculation in dichloromethane.

Table 1 Gibbs free energy of activation $\Delta\Delta G^{\neq}$ (kJ mol^{-1}), branching ratio of *anti* conformer *versus* experimental results

	Theory (gas phase)		Theory (dichloromethane)		Experiment[16]
	$\Delta\Delta G^{\neq}$	Ratio	$\Delta\Delta G^{\neq}$	Ratio	Ratio
Benzaldehyde	11.11	88 : 1	11.39	99 : 1	100 : 0

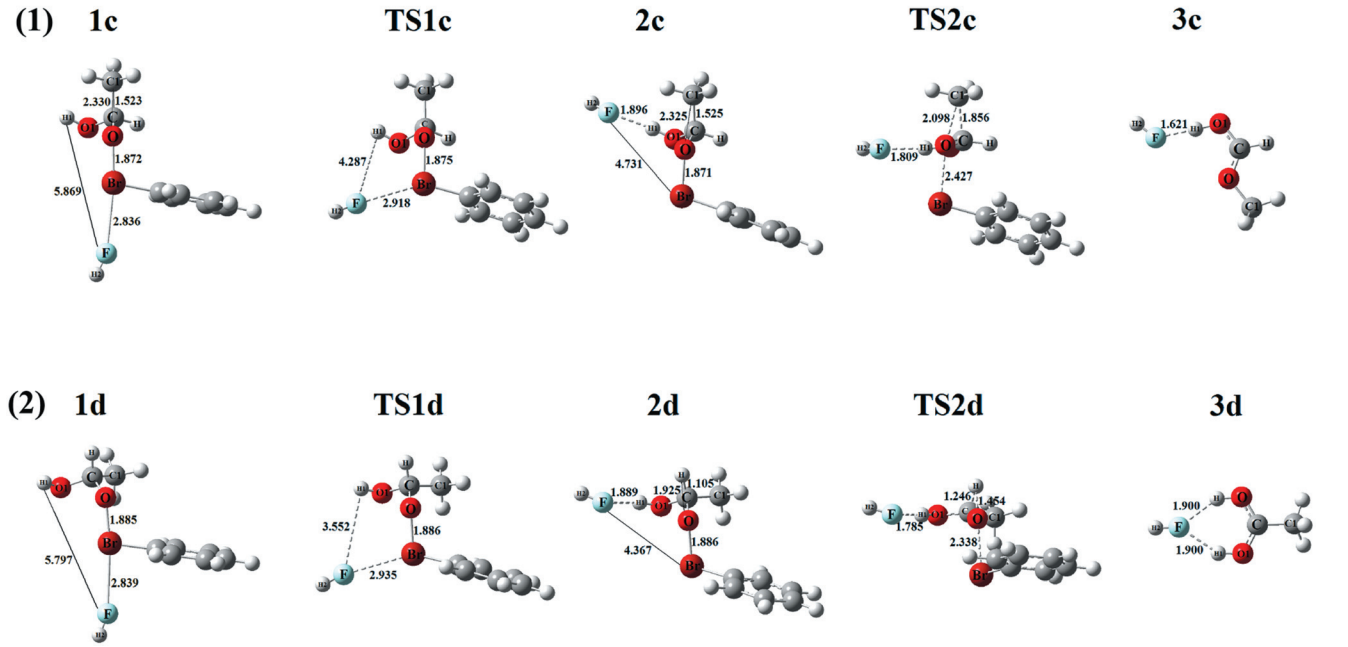

Fig. 5 Structures of intermediates, transition states, and products of the stepwise mechanism of protonated *anti*-α-hydroxyethoxy-λ^3-bromane, using DFT (B3LYP/6-31++G**) methods: CH_3 migration (above) and hydrogen migration (below). **1c**(**1d**): protonated *anti*-α-hydroxyethoxy-λ^3-bromane, **3c**(**3d**): complex of HF and protonated $HCOOCH_3$ (CH_3COOH). The distances are in Å.

calculation with CCSD(T) method was used, the results show the same trend with the B3LYP method. All these results confirm that B3LYP is more suitable for description of the BVO reaction than MP2, which is consistent with ref. 9. Additionally, the β-elimination process was also considered as suggested by Ochiai and coworkers in this part, but no reasonable results were obtained.

3.3.2 Concerted mechanism of protonated α-hydroxyethoxy-λ^3-bromane. For the *anti* conformer, Fig. 4 and 6 display the free energy profile and all of the main structures in the concerted mechanism. As can be seen in Fig. 4, the hydrogen shift (green line) requires a free energy of activation of about 42.87 kJ mol^{-1}, which is 9.69 kJ mol^{-1} lower than the methyl shift (blue line). It indicates that the hydrogen shift is easier than the methyl shift, which is compatible with the experimental data of the preferred formation of acetic acid over methyl formate.[16] The reason for the results has been interpreted in the stepwise mechanism.

For either the methyl or the hydrogen migration in the BVO reaction of acetaldehyde, the stepwise mechanism is more favorable than the concerted mechanism. It illustrates that α-hydroxyethoxy-λ^3-bromane is more likely to form in the stepwise mechanism. The results can also be explained by the NPA charge analysis. The charge on oxygen (in structure **2c**) in the stepwise mechanism is −0.567, which is more positive than that on oxygen (−0.578) in structure **1c** for the concerted mechanism. Therefore, the methyl shift in the stepwise mechanism is easier than the concerted mechanism. Similarly, this can also explain why the hydrogen shift in the stepwise mechanism is more liable to occur. Thus, for α-hydroxyethoxy-λ^3-bromane in BVO of acetaldehyde, the stepwise mechanism of the *anti* conformer is favorable.

It is interesting that the same two mechanisms occurring on acetaldehyde and benzaldehyde show different priorities. In both cases, the stepwise mechanism is advantageous for the hydrogen migration and methyl migration. In the above sections, we have explained this phenomenon by charge analysis. However, for the phenyl migration, the concerted mechanism is competitive with the stepwise mechanism. Here, some difference between methyl and phenyl migration can be found by analyzing the geometrical parameters. For the phenyl migration, as to the leaving group, PhBr, the Br···O distance change in the concerted mechanism is larger than that in the stepwise mechanism, as 2.35 Å (TSa) > 2.22 Å (TS2a). As to the migrating group, the same trend of *d*(C1–O) (1.87 Å (TSa) < 1.98 Å (TS2a)) can be found. For the methyl migration, *d*(Br–O) and *d*(C1–O) changes little (2.43 Å (TS2c) and 2.49 Å (TSc) and 2.10 Å (TS2c) and 2.08 Å (TSc), respectively). That is to say, the concerted mechanism in phenyl migration has a stronger effect than in methyl migration. Based on the charge and geometrical parameter analysis, the stepwise mechanism does not show priority in phenyl migration.

To better explain the experimental results, the solvent effect was also examined with dichloromethane, as can be seen in Fig. 4 (the values in parentheses). For either the stepwise or the concerted mechanism, the required free energy of activation for the hydrogen migration is lower than that for the methyl migration, which indicates that the hydrogen shift is easier than the methyl shift in dichloromethane. All the results in solvent are consistent with those in the gas phase, and are compatible with the experimental values.[16]

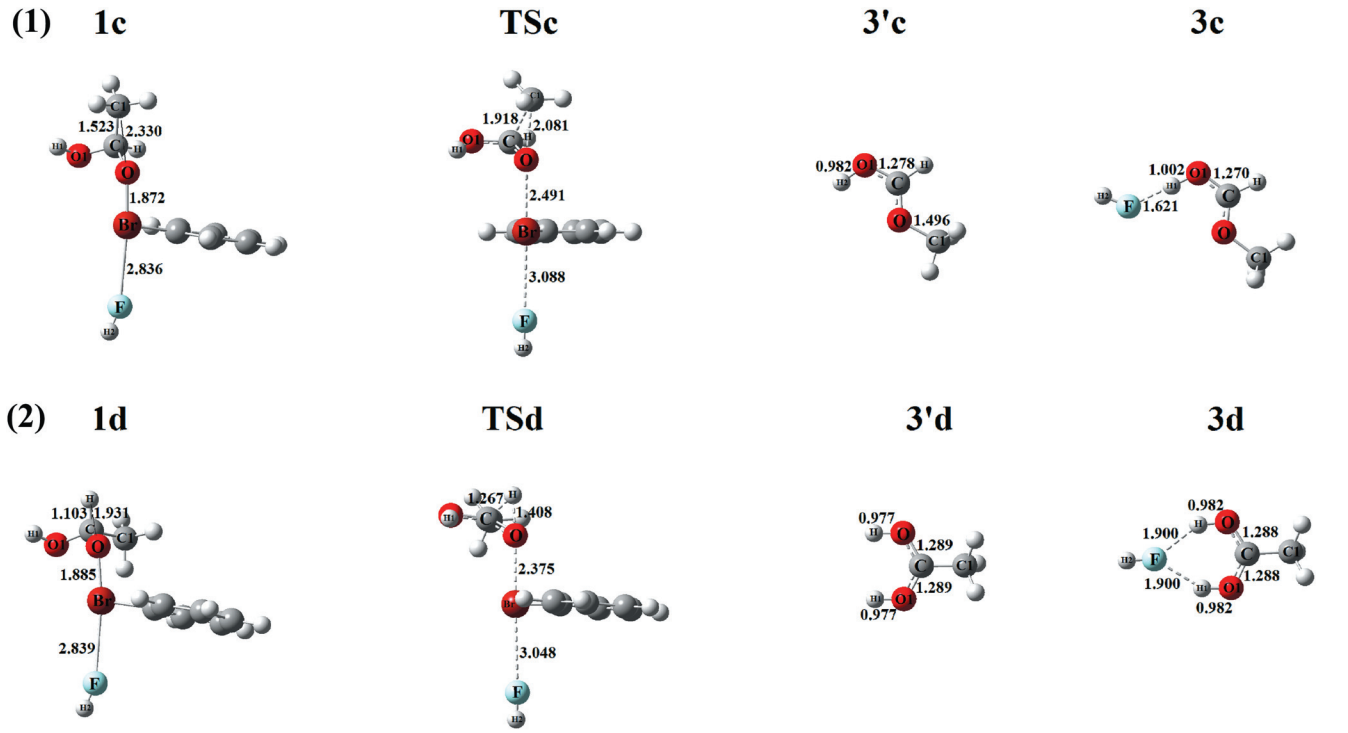

Fig. 6 Structures of intermediates, transition states, and products of concerted mechanism of protonated *anti*-α-hydroxyethoxy-λ^3-bromane, using DFT (B3LYP/6-31++G**) methods: CH_3 migration (above) and hydrogen migration (below). **1c**(**1d**): protonated *anti*-α-hydroxyethoxy -λ^3-bromane, **3c**(**3d**): complex of HF and protonated $HCOOCH_3$ (CH_3COOH). The distances are in Å.

Table 2 Gibbs free energy of activation $\Delta\Delta G^{\neq}$ (kJ mol^{-1}), branching ratio of *anti* conformer *versus* Experimental results

	Theory (gas phase)		Theory (dichloromethane)		Experiment[16]
	$\Delta\Delta G^{\neq}$	Ratio	$\Delta\Delta G^{\neq}$	Ratio	Ratio
Acetaldehyde	8.00	25 : 1	6.97	17 : 1	95 : 5 (19 : 1)

Additionally, the *syn* conformers were also examined (see Fig. S4–S6†). All of the calculated results indicate the same trend of moiety migration as in the *anti* conformer. Comparing the *syn* conformer with the *anti* one, the latter is advantageous in both mechanisms.

3.3.3 Rate constants and branching ratio. To better understand the migration step, the rate constants were also examined for the favorable mechanism in dichloromethane by TST theory given in the calculation details at 298.15 K. For the methyl shift, the forward rate constant is 5.61×10^5 s^{-1}, while the reverse rate constant is 4.47×10^{-39} mol^{-1} dm^3 s^{-1}. For the hydrogen shift, the forward rate constant is 9.33×10^6 s^{-1}, while the reverse rate constant is 5.30×10^{-51} mol^{-1} dm^3 s^{-1}. For both the methyl and the hydrogen shift, the reverse reaction is very difficult to undertake, and it is found that the reaction rate constant of CH_3COOH formation is about twenty times higher than that of $HCOOCH_3$ formation.

Additionally, the differences in the calculated Gibbs free energy of activation ($\Delta\Delta G^{\neq}$) have been used to predict the product yield from absolute rate theory, by $\ln(k_{CH3COOH}/k_{HCOOCH3}) = \Delta\Delta G^{\neq}/RT$, in order to further verify the reliability of our theoretical results. Table 2 lists the corresponding $\Delta\Delta G^{\neq}$ and branching ratio in the gas phase and in dichloromethane. Compared with experimental values, it is found that our computational results are obviously in excellent agreement with the experimental observation.[16]

Conclusion

For the key step of the new-type BVO reaction, all the reactive channels of the new Criegee intermediate, including *anti* and *syn* conformers of two optical isomers, have been studied by using DFT methods at the B3LYP/6-31++G** computational level. Two different mechanisms (stepwise and concerted) have been examined. Our calculations confirm that the stepwise mechanism of the *anti* conformer has superiority for this novel BVO reaction (except for the phenyl migration of benzaldehyde). For benzaldehyde, whether in the gas phase or in dichloromethane, the much lower free energy barrier of the phenyl shift resulted in the predominating product being PhOCOH. However for acetaldehyde, the hydrogen shift occurs more readily than the methyl shift. As a consequence, CH_3COOH was proved to be

the major product. The calculated branching ratios are in good agreement with the experimental results. The calculated rate constants also indicate the same trend.

Acknowledgements

This work is supported by the Fundamental Research Funds for the Central Universities (10CX04020A), the National Important Scientific Foundation (2008ZX05026-004-05), the National Natural Science Foundation of China (No. 21103096) and the Natural Science Foundation of Shandong Province (ZR2010BM024). We also thank the Project of Shandong Province Higher Educational Science and Technology Program, China (No. J10LB06).

References

1 A. Baeyer and V. Villiger, *Ber. Dtsch. Chem. Ges.*, 1899, **32**, 3625.
2 G. R. Krow, *Org. React.*, 1993, **43**, 251.
3 M. Renz and B. Meunier, *Eur. J. Org. Chem.*, 1999, 737.
4 G. J. ten Brink, I. W. C. E. Arends and R. A. Sheldon, *Chem. Rev.*, 2004, **104**, 4105.
5 F. Grein, A. C. Chen, D. Edwards and C. M. Crudden, *J. Org. Chem.*, 2006, **71**, 861.
6 S. Yamabe and S. Yamazaki, *J. Org. Chem.*, 2007, **72**, 3031.
7 J. R. Alvarez-Idaboy, L. Reyes and J. Cruz, *Org. Lett.*, 2006, **8**, 1763.
8 J. R. Alvarez-Idaboy and L. Reyes, *J. Org. Chem.*, 2007, **72**, 6580.
9 J. R. Alvarez-Idaboy, L. Reyes and N. Mora-Diez, *Org. Biomol. Chem.*, 2007, **5**, 3682.
10 L. Reyes, J. R. Alvarez-Idaboy and N. Mora-Diez, *J. Phys. Org. Chem.*, 2009, **22**, 643.
11 N. Mora-Diez, S. Keller and J. R. Alvarez-Idaboy, *Org. Biomol. Chem.*, 2009, **7**, 3682.
12 R. Criegee, *Justus Liebigs Ann. Chem.*, 1948, **560**, 127.
13 A. Corma, L. T. Nemeth, M. Renz and S. Valencia, *Nature*, 2001, **412**, 423.
14 P. A. Smith, in *Molecular Rearrangements*, ed. P. de Mayo, Interscience, New York, 1963, vol. 1.
15 C. Lethtinen, V. Nevalainen and G. Brunow, *Tetrahedron*, 2000, **56**, 9375.
16 M. Ochiai, A. Yoshimura, K. Miyamoto, S. Hayashi and W. Nakanishi, *J. Am. Chem. Soc.*, 2010, **132**, 9236.
17 M. J. Frisch, G. W. Trucks, H. B. Schlegel, G. E. Scuseria, M. A. Robb, J. R. Cheeseman, J. A. Montgomery Jr., T. Vreven, K. N. Kudin, J. C. Burant, J. M. Millam, S. S. Iyengar, J. Tomasi, V. Barone, B. Mennucci, M. Cossi, G. Scalmani, N. Rega, G. A. Petersson, H. Nakatsuji, M. Hada, M. Ehara, K. Toyota, R. Fukuda, J. Hasegawa, M. Ishida, T. Nakajima, Y. Honda, O. Kitao, H. Nakai, M. Klene, X. Li, J. E. Knox, H. P. Hratchian, J. B. Cross, V. Bakken, C. Adamo, J. Jaramillo, R. Gomperts, R. E. Stratmann, O. Yazyev, A. J. Austin, R. Cammi, C. Pomelli, J. Ochterski, P. Y. Ayala, K. Morokuma, G. A. Voth, P. Salvador, J. J. Dannenberg, V. G. Zakrzewski, S. Dapprich, A. D. Daniels, M. C. Strain, O. Farkas, D. K. Malick, A. D. Rabuck, K. Raghavachari, J. B. Foresman, J. V. Ortiz, Q. Cui, A. G. Baboul, S. Clifford, J. Cioslowski, B. B. Stefanov, G. Liu, A. Liashenko, P. Piskorz, I. Komaromi, R. L. Martin, D. J. Fox, T. Keith, M. A. Al-Laham, C. Y. Peng, A. Nanayakkara, M. Challacombe, P. M. W. Gill, B. G. Johnson, W. Chen, M. W. Wong, C. Gonzalez and J. A. Pople, *GAUSSIAN 03*, Gaussian, Inc., Wallingford, CT, 2004.
18 A. D. Backe, *J. Chem. Phys.*, 1993, **98**, 1372.
19 A. D. Backe, *J. Chem. Phys.*, 1993, **98**, 5648.
20 A. D. Becke, *Phys. Rev. A*, 1988, **38**, 3098.
21 C. Lee, W. Yang and R. G. Parr, *Phys. Rev. B*, 1988, **37**, 785.
22 V. Barone and M. Cossi, *J. Phys. Chem. A*, 1998, **102**, 1995.
23 V. Barone, M. Cossi and J. Tomasi, *J. Comput. Chem.*, 1998, **19**, 404.
24 A. K. Rappé, C. J. Casewit, K. S. Colwell and W. A. Goddard, *J. Am. Chem. Soc.*, 1992, **114**, 10024.
25 A. Marini, S. Macchi, S. Jurinovich, D. Catalano and B. Mennucci, *J. Phys. Chem. A*, 2011, **115**, 10035.
26 A. E. Reed, L. A. Curtiss and F. Weinhold, *Chem. Rev.*, 1988, **88**, 899.
27 J. E. Carpenter and F. Weinhold, *J. Mol. Struct. (THEOCHEM)*, 1988, **169**, 41.
28 J. P. Foster and F. Weinhold, *J. Am. Chem. Soc.*, 1980, **102**, 7211.
29 A. E. Reed and F. Weinhold, *J. Chem. Phys.*, 1983, **78**, 4066.
30 A. E. Reed, R. B. Weinstock and F. Weinhold, *J. Chem. Phys.*, 1985, **83**, 735.
31 J. A. Pople, M. Head-Gordon and K. J. Raghavachari, *Chem. Phys.*, 1987, **87**, 5968.
32 K. Kongpatpanich, T. Nanok, B. Boekfa, M. Probst and J. Limtrakul, *Phys. Chem. Chem. Phys.*, 2011, **13**, 6462.
33 D. G. Truhlar, B. C. Garrett and S. J. Klippenstein, *J. Phys. Chem.*, 1996, **100**, 12771.
34 R. W. Taft, in *Steric Effects in Organic Chemistry*, ed. M. S. Newman, Wiley, New York, 1956.
35 M. A. Winnik and V. Stoute, *Can. J. Chem.*, 1973, **51**, 2788.

